

Triheteromeric NR1/NR2A/NR2B Receptors Constitute the Major *N*-Methyl-D-aspartate Receptor Population in Adult Hippocampal Synapses

Received for publication, September 7, 2010, and in revised form, November 18, 2010. Published, JBC Papers in Press, December 29, 2010, DOI 10.1074/jbc.M110.182600

Claudia Rauner and Georg Köhr¹

From the Department of Molecular Neurobiology, Max-Planck-Institute for Medical Research, Jahnstrasse 29, D-69120 Heidelberg, Germany

NMDA receptors (NMDARs), fundamental to learning and memory and implicated in certain neurological disorders, are heterotetrameric complexes composed of two NR1 and two NR2 subunits. The function of synaptic NMDARs in postnatal principal forebrain neurons is typically attributed to diheteromeric NR1/NR2A and NR1/NR2B receptors, despite compelling evidence for triheteromeric NR1/NR2A/NR2B receptors. In synapses, the properties of triheteromeric NMDARs could thus far not be distinguished from those of mixtures of diheteromeric NMDARs. To find a signature of NR1/NR2A/NR2B receptors, we have employed two gene-targeted mouse lines, expressing either NR1/NR2A or NR1/NR2B receptors without NR1/NR2A/NR2B receptors, and compared their synaptic properties with those of wild type. In acute hippocampal slices of mutants older than 4 weeks we found a distinct voltage dependence of NMDA R-mediated excitatory postsynaptic current (NMDA EPSC) decay time for the two diheteromeric NMDARs. In wild-type mice, NMDA EPSCs unveiled the NR1/NR2A characteristic for this voltage-dependent deactivation exclusively, indicating that the contribution of NR1/NR2B receptors to evoked NMDA EPSCs is negligible in adult CA3-to-CA1 synapses. The presence of NR1/NR2A/NR2B receptors was obvious from properties that could not be explained by a mixture of diheteromeric NR1/NR2A and NR1/NR2B receptors or by the presence of NR1/NR2A receptors alone. The decay time for NMDA EPSCs in wild type was slower than that for NR1/NR2A receptors, and the sensitivity of NMDA EPSCs to NR2B-directed NMDAR antagonists was 50%. Thus, NR2B is prominent in adult hippocampal synapses as an integral part of NR1/NR2A/NR2B receptors.

Among ionotropic glutamate receptors, the function of NMDA receptors (NMDARs)² is unique because of the requirement of simultaneous agonist/co-agonist binding and because of a highly Ca^{2+} -permeable pore, which is controlled in a voltage-dependent manner. The voltage-dependent Mg^{2+} block enables NMDARs to detect presynaptic glutamate release and postsynaptic depolarization through somatic or dendritic spikes. NMDARs are therefore coincidence detectors of pre-

and postsynaptic activity. Their function is related to the induction of synaptic plasticity, various forms of learning and memory, and several pathophysiological processes (1–3).

Two glycine/serine-binding NR1 (GluN1) and two glutamate-binding NR2 (GluN2) subunits presumably form heterotetrameric NR1/NR2 complexes in which the NR1 subunits assemble diagonally to each other (4, 5). NR1 shows continuous and ubiquitous expression in the brain, whereas expression of the four NR2 subunit genes, NR2A–D, is temporally and spatially regulated (6, 7). The expression of NR2A and NR2C starts after birth in the forebrain and cerebellum, respectively, whereas NR2B and NR2D are present already during embryonic development. In the hippocampus, NR2C immunoreactivity cannot be detected throughout development (6, 8), and NR2D expression decreases postnatally (6) and appears to be confined to extrasynaptic sites under basal synaptic conditions (9–11). By contrast, NR2B can be detected in postsynaptic densities of adult mice by protein isolation, subcellular fractionation, and immunogold labeling (12–14), and NR2B expression is relatively constant within hippocampal CA1 regardless of postsynaptic density size (15). The NR2 subunits endow NMDARs with distinct biophysical and pharmacological properties, including deactivation, open probability, strength of Mg^{2+} block, single-channel conductance, and sensitivity to extracellular allosteric modulators (1, 16, 17).

Diheteromeric NR1/NR2 receptors have been studied intensively in heterologous systems and in cultured neurons, identifying NR2 subunit-specific synthesis, trafficking, and degradation pathways (for a recent review, see Ref. 18). In contrast, NR2 subunit-specific roles in the induction of synaptic plasticity (for review, see Ref. 19) or excitotoxicity (20–22) remain inconclusive, especially in neuronal preparations, which contain di- and triheteromeric NMDARs as demonstrated by many studies (23–29). The presence of two different NR2 subunits within triheteromeric NMDARs could lead to unique receptor properties, expanding the repertoire of diheteromeric NMDAR signaling. Triheteromeric NMDARs are difficult to isolate biochemically because of the low level of solubility, especially in older animals (29) and electrophysiologically because of the difficulty to access single-channel conductances of synaptic NMDARs, leaving their abundance, properties, and function ambiguous.

Expression of NR1, NR2A, and NR2B in adult CA1 pyramidal cells leads to the formation of NR1/NR2A, NR1/NR2B, and NR1/NR2A/NR2B receptors. Here, we provide evidence that

¹ To whom correspondence should be addressed. Fax: 49-6221-486110; E-mail: kohl@mpimf-heidelberg.mpg.de.

² The abbreviations used are: NMDAR, NMDA receptor; ACSF, artificial cerebrospinal fluid; EPSC, excitatory postsynaptic current; LTP, long-term potentiation; ICP, inductive coupled.

NR1/NR2A/NR2B receptors constitute the major NMDAR population in adult CA3-to-CA1 synapses. We analyzed subtype-specific characteristics of diheteromeric NMDARs in acute slices of adult mice in which either NR2A was constitutively ablated (*NR2A*^{-/-}) (30), or NR2B was selectively removed from principal forebrain neurons (*NR2B*^{ΔFb}) (31). In both mouse lines, the expression of other NR2 subunits was not found to be noticeably affected. This genetic approach combined with the use of pharmacology in wild-type mice allowed us to decipher the synaptic NMDAR composition in CA1 neurons and may help to identify NMDAR subtypes in other brain regions.

EXPERIMENTAL PROCEDURES

All experimental procedures were in accordance with the animal welfare guidelines of the Max Planck Society. Deeply anesthetized (isoflurane) *NR2A*^{-/-} mice (30) (neonatal, P4–P6; adult, P27–P48), *NR2B*^{ΔFb} mice (31) (adult, P41–P48) and age-matched wild-type mice (WT, C57BL/6) were decapitated and their brains were removed. Transverse or coronal hippocampal slices (250 μm) were prepared at 4 °C, recovered for 1 h at 35 °C, and maintained at room temperature (22–25 °C) in artificial cerebrospinal fluid (ACSF) containing 125 mM NaCl, 25 mM NaHCO₃, 2.5 mM KCl, 1.25 mM NaH₂PO₄, 1 mM MgCl₂, 25 glucose, 2 mM CaCl₂; bubbled with 95% O₂/5% CO₂ (pH 7.3, 320 mOsm). Single slices were transferred to the recording chamber and perfused continuously with ACSF containing 10 μM bicuculline methiodide or 5 μM gabazine, 10 μM NBQX, and 10 μM glycine. Cells were visualized using an upright Zeiss Axioskop (Goettingen, Germany). Whole cell recordings were performed at room temperature, using patch pipettes pulled from borosilicate glass capillaries with resistances of 3.5–6.5 megohms when filled with 125 mM cesium gluconate, 20 mM CsCl, 10 mM NaCl, 10 mM HEPES, 0.2 mM EGTA, 4 mM MgATP, 0.3 mM Na₃GTP, 2.5 mM QX-314Cl (pH 7.3, 270–320 mOsm). Liquid junction potential was not corrected. Series and input resistances were monitored continuously by measuring peak and steady-state currents in response to hyperpolarizing pulses (–5 mV, 20 ms), and cells were excluded if series resistance changed by >20%.

Pharmacologically isolated NMDA EPSCs were evoked in CA1 pyramidal cells by electrical stimulation of Schaffer collaterals at 0.1 Hz in stratum radiatum about 150 μm distant from the CA1 cell body layer with monopolar glass pipettes filled with 1 M NaCl. NMDA EPSCs were recorded at –40 and +40 mV in the presence of 1 mM Mg²⁺ (ACSF) or following 25 min of Mg²⁺ washout using nominally Mg²⁺-free ACSF: 125 mM NaCl, 25 mM NaHCO₃, 2.5 mM KCl, 1.25 mM NaH₂PO₄, 25 mM glucose, 2 mM CaCl₂ (pH 7.3, 310 mOsm). During Mg²⁺ washout, electrical stimulation was preserved at 0.1 Hz. The Mg²⁺ concentration was determined to be 1.5 μM in freshly prepared Mg²⁺-free ACSF and ≤4.5 μM in ACSF collected following 25 min of slice perfusion (ICP-optical emission spectrometry by Christian Scholz, University of Heidelberg). In some experiments, the NMDAR antagonist D-APV (Biotrend) or one of the two NR2B-directed antagonists CP-101,606 (Pfizer) or ifenprodil (Sigma) was present. NR2B-directed NMDAR antagonists were washed in for 20 min either in the presence or

absence of Mg²⁺ before their effects on NMDA EPSCs were determined. Synaptic responses were filtered at 3 kHz and digitized at 10 kHz using the patch clamp amplifier EPC-9 (HEKA, Lambrecht, Germany), which was controlled by Pulse/Patchmaster software. Visually identified polysynaptic NMDA EPSCs were excluded, and monosynaptic currents were averaged over 1.5 min of recording. The programs Pulsefit/Fitmaster were used for off-line analysis of peak amplitudes and decay time. Averaged NMDA EPSCs were fitted biexponentially (32). These biphasic decay times reflect kinetic heterogeneity rather than NMDAR subtype heterogeneity (33). To compare decay times between genotypes weighted Taus (ms) were calculated using the formula $\text{Tau}_{\text{weighted}} = (I_{\text{fast}}/I_{\text{fast}} + I_{\text{slow}}) * \text{Tau}_{\text{fast}} + (I_{\text{slow}}/I_{\text{slow}} + I_{\text{fast}}) * \text{Tau}_{\text{slow}}$, where *I* is the amplitude of the fast or slow component, and Tau is the respective decay time constant (32). For each cell, at least two $\text{Tau}_{\text{weighted}}$ were averaged for each recording condition, before the voltage dependence of decay was estimated by the ratio $\text{Tau}_{\text{weighted}}$ at –40 mV divided by $\text{Tau}_{\text{weighted}}$ at +40 mV. Data are presented as mean ± S.E. Statistical significance was evaluated by paired (#) or unpaired (†) Student's *t* tests and ANOVA with Fisher's least squares difference post hoc analysis (*). *p* < 0.05 was regarded as significant.

RESULTS

Amplitudes of NMDA EPSCs Mediated via Distinct NMDAR Subtypes Are Similarly Sensitive to Mg²⁺—Agonist-evoked currents mediated by recombinant NR1/NR2A receptors deactivate 3–4-fold faster than those mediated by recombinant NR1/NR2B receptors (1, 34), whereas their sensitivity to extracellular Mg²⁺ is similar (6, 35). To investigate the sensitivity to Mg²⁺ for different synaptic NMDAR subtypes in acute slices, we compared the amplitudes of NMDA EPSCs recorded at –40 and +40 mV in hippocampal CA1 neurons before and after washout of external Mg²⁺. Diheteromeric NR1/NR2B receptors were investigated in *NR2A*^{-/-} mice (30), and diheteromeric NR1/NR2A receptors in conditional *NR2B*^{ΔFb} mice (31) to avoid perinatal lethality from complete NR2B knock-out (36). Di- and triheteromeric NMDARs were investigated in wild-type mice.

In *NR2B*^{ΔFb} mice, NR2B is progressively removed over the first 3 postnatal months from principal forebrain neurons, including CA1 pyramidal cells. Consequently, 36 of 79 CA1 neurons recorded in slices from *NR2B*^{ΔFb} mice showed NMDA EPSCs with fast decay times (<39 ms in 1 mM Mg²⁺ at –40 mV) not observed in wild type (39–87 ms, *n* = 37). A subset of the 36 cells from the *NR2B*^{ΔFb} mice was used for this project (19–29 ms, *n* = 9; Table 1). This fast decay time and the concurrent insensitivity of NMDA EPSCs to the NR2B-directed NMDAR antagonist CP-101,606 (10 μM; data not shown) confirmed that the NMDA EPSCs that we selected from *NR2B*^{ΔFb} mice were exclusively mediated via NR1/NR2A receptors. For all three genotypes, Mg²⁺ washout increased 3–4-fold the amplitudes of NMDA EPSCs at –40 mV, whereas changes of amplitudes at +40 mV were negligible (Fig. 1*A* and *B*). Thus, the sensitivity to Mg²⁺ block is comparable for synaptic NMDARs of the three genotypes.

TABLE 1

Deactivation kinetics and sensitivity to CP-101,606 (10 μ M) for NMDA EPSCs recorded in CA1 neurons of wild-type, *NR2A*^{−/−}, and *NR2B*^{ΔFb} mice at −40 and +40 mV in the presence and absence of Mg²⁺

The decay time constants and the −40 mV/+40 mV ratios were determined between P27 and P48. For each genotype, # indicates significance following Mg²⁺ washout for decay time or between 1 and 0 mM Mg²⁺ for experiments with CP-101,606 (#, *p* < 0.05 and ##, *p* < 0.001); † indicates significance between −40 and +40 mV regarding decay time (†, *p* < 0.05 and ††, *p* < 0.0001); * indicates significance between P5 and P27–P48 (*, *p* < 0.05; **, *p* < 0.01; and ***, *p* < 0.0001). Compared with both NR2 mutants, NMDA EPSC decay time in wild type was distinct (*p* < 0.0001) but not halfway. For statistics between genotypes, see figures and text. The number of cells is indicated in parentheses.

Genotype	Analysis of	Membrane potential	1 mM Mg ²⁺		0 mM Mg ²⁺	
		<i>mV</i>	<i>ms</i>	<i>ratio</i>	<i>ms</i>	<i>ratio</i>
WT	Decay time	−40	54 ± 1.67 (37)	0.46 ± 0.01 (37)	97 ± 5.71## (37)	0.69 ± 0.04 (37)
		+40	119 ± 3.30†† (37)		148 ± 8.99##,†† (37)	
<i>NR2A</i> ^{−/−}	Decay time	−40	233 ± 18.60 (9)	0.76 ± 0.05 (9)	306 ± 16.64# (9)	1.02 ± 0.03 (9)
		+40	307 ± 16.18† (9)		302 ± 18.32 (9)	
<i>NR2B</i> ^{ΔFb}	Decay time	−40	25 ± 1.20 (9)	0.49 ± 0.03 (9)	34 ± 3.24# (9)	0.60 ± 0.05 (9)
		+40	52 ± 2.94†† (9)		57 ± 3.54†† (9)	
			P5 (%)	P27-P48 (%)	P5 (%)	P27-P48 (%)
WT	Reduction by CP-101,606	−40	57 ± 5.19 (7)	14 ± 4.45*** (7)	68 ± 2.89 (6)	55 ± 4.08##,* (9)
		+40	46 ± 5.35 (7)	17 ± 5.39** (7)	62 ± 2.80# (6)	52 ± 3.44# (9)
<i>NR2A</i> ^{−/−}	Reduction by CP-101,606	−40		50 ± 5.41 (7)		80 ± 3.83## (7)
		+40		40 ± 7.86 (7)		75 ± 4.53# (7)

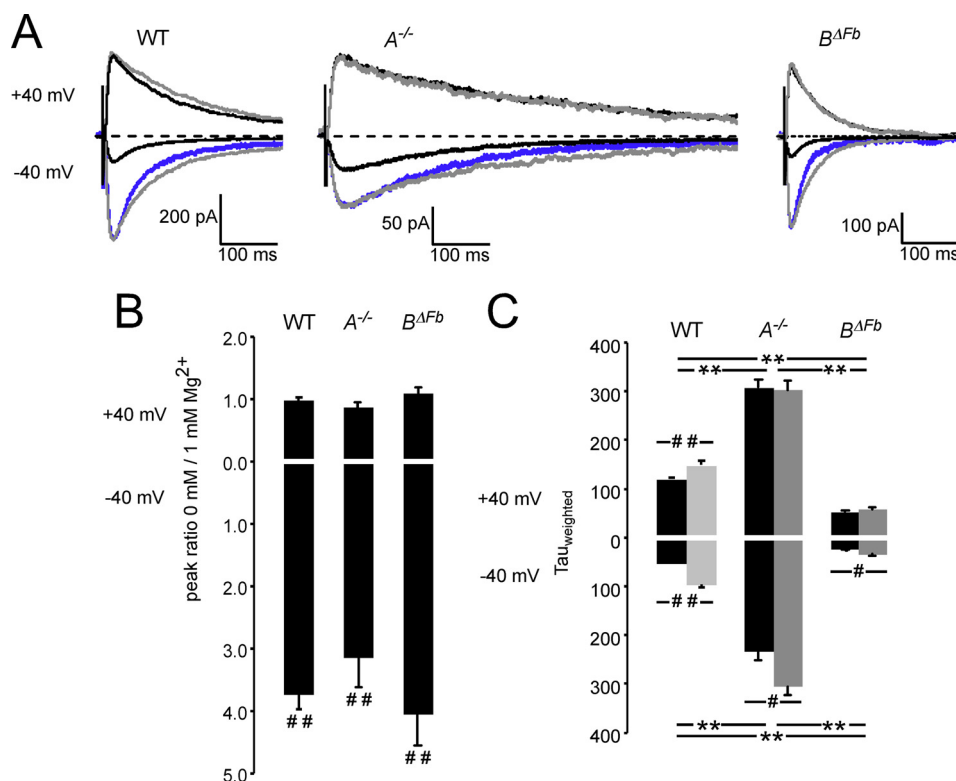


FIGURE 1. Mg²⁺ sensitivity of amplitudes and of deactivation kinetics of NMDA EPSCs in adult wild-type, *NR2A*^{−/−}, and *NR2B*^{ΔFb} mice. A, representative averaged current traces of pharmacologically isolated NMDA EPSCs (GABA_AR and AMPAR antagonists) recorded in CA1 cells before (black) and after (gray) Mg²⁺ washout for wild-type, *NR2A*^{−/−}, and *NR2B*^{ΔFb} mice. Blue traces at −40 mV show black traces scaled to the amplitude of gray traces. B, bars showing peak ratios of NMDA EPSCs and illustrating effects of Mg²⁺ washout on amplitudes at −40 mV (downward) and +40 mV (upward). The basis of the bars at 0 is marked by a white line. At −40 mV, NMDA EPSCs similarly (*p* = 0.35, ANOVA) increased 3–4-fold (WT, 3.77 ± 0.24, *n* = 32, ##, *p* < 0.0001 paired *t* test; *NR2A*^{−/−} mice, 3.16 ± 0.48, *n* = 9, ##, *p* < 0.001; *NR2B*^{ΔFb}, 4.12 ± 0.51, *n* = 7, ##, *p* < 0.001). At +40 mV, NMDA EPSCs remained unchanged (WT, 0.97 ± 0.05, *n* = 32, *p* = 0.31; *NR2A*^{−/−}, 0.86 ± 0.07, *n* = 9, *p* = 0.08; *NR2B*^{ΔFb}, 1.07 ± 0.09, *n* = 7, *p* = 0.34), and the changes at −40 mV were not different between genotypes (*p* = 0.31 ANOVA). C, bars show averaged decay time constants (Tau_{weighted}) of NMDA EPSCs in the presence (black bars) and absence (gray bars) of Mg²⁺ at −40 mV (downward) and +40 mV (upward). Compared with wild type, NMDA EPSCs were slower in *NR2A*^{−/−} mice and faster in *NR2B*^{ΔFb} mice (**, *p* < 0.0001 ANOVA). At −40 mV, decay changes caused by Mg²⁺ washout were more pronounced in wild type than in the two NR2 mutants (WT, 80.83 ± 8.72%, *n* = 37, ##, *p* < 0.0001; *NR2A*^{−/−}, 37.47 ± 13.66%, *n* = 9, #, *p* < 0.01; *NR2B*^{ΔFb}, 36.50 ± 11.73%, *n* = 9, #, *p* < 0.05). At +40 mV, decay changes occurred exclusively in wild type (WT, 23.12 ± 5.67%, *n* = 37, ##, *p* < 0.001; *NR2A*^{−/−}, 0.60 ± 6.01%, *n* = 9, *p* = 0.77; *NR2B*^{ΔFb}, 11.01 ± 5.48%, *n* = 9, *p* = 0.10).

Mg²⁺ Sensitivity of NMDA EPSC Decay Time Reveals Presence of NR1/NR2A/NR2B Receptors in Synapses of Adult Wild-type Mice—Consistent with recombinant diheteromeric NMDARs (6, 16, 34), NR1/NR2B receptor-mediated NMDA EPSCs in CA1 synapses of *NR2A*^{−/−} mice decayed significantly slower than NR1/NR2A receptor-mediated NMDA EPSCs in

NR2B^{ΔFb} mice (approximately 9-fold slower at −40 mV and about 6-fold slower at +40 mV; Fig. 1C and Table 1). This difference was observed in the presence of Mg²⁺ as well as following washout of Mg²⁺, which prolonged the decay time constants of NMDA EPSCs, consistent with previous findings (37). In wild-type mice, the decay time of NMDA EPSCs was

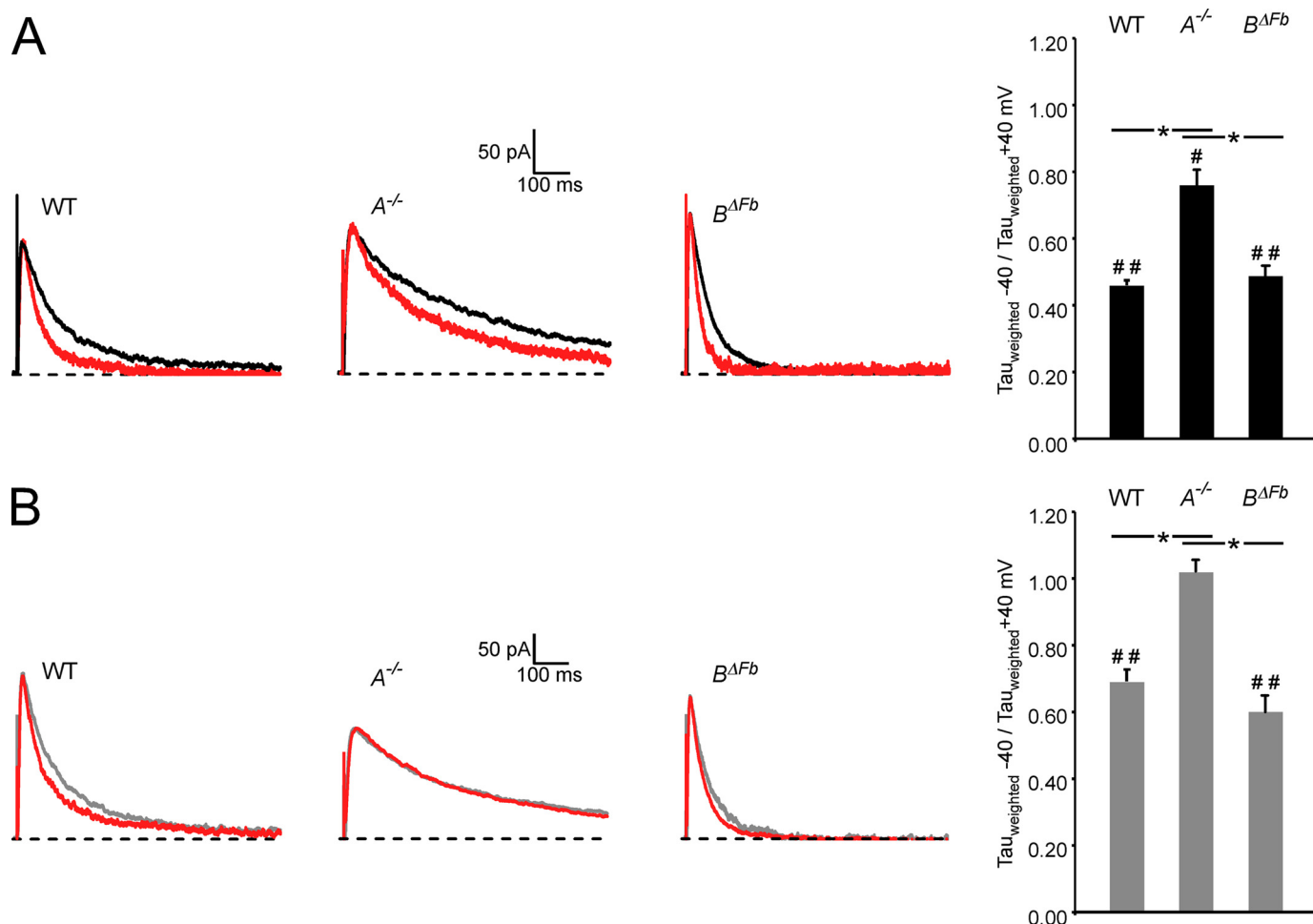


FIGURE 2. Voltage dependence of NMDA EPSC deactivation kinetics in adult wild-type, NR2A^{-/-}, and NR2B^{ΔFb} mice. Averaged representative current traces show NMDA EPSCs at +40 mV in black (A, normal Ringer's solution containing 1 mM Mg²⁺) or in gray (B, Mg²⁺-free Ringer's solution), and NMDA EPSCs recorded at -40 mV were inverted and scaled to EPSCs at +40 mV in red. A, bar diagram shows the ratio of Tau_{weighted} -40/Tau_{weighted} +40 mV in the presence of 1 mM Mg²⁺ (WT, 0.46 ± 0.01, n = 37, ##, p < 0.0001; NR2A^{-/-}, 0.76 ± 0.05, n = 9, #, p < 0.05; NR2B^{ΔFb}, 0.49 ± 0.03, n = 9, ##, p < 0.0001). Voltage dependence of decay was reduced in NR2A^{-/-} mice compared with wild-type and NR2B^{ΔFb} mice (*, p < 0.01 ANOVA) and was similar in wild-type and NR2B^{ΔFb} mice (p > 0.05 ANOVA). B, same as A, but in the absence of Mg²⁺ (WT, 0.69 ± 0.04, n = 37, ##, p < 0.0001; NR2A^{-/-}, 1.02 ± 0.03, n = 9, p = 0.94; NR2B^{ΔFb}, 0.60 ± 0.05, n = 9, ##, p < 0.0001). The Mg²⁺-independent voltage dependence of decay in wild-type and NR2B^{ΔFb} mice was different from NR2A^{-/-} mice (*, p < 0.01 ANOVA) and was similar in wild-type and NR2B^{ΔFb} mice (p > 0.05 ANOVA).

distinct ($p < 0.0001$ ANOVA) and intermediate but not halfway compared with that in both NR2 mutant mouse lines.

Notably in dentate gyrus granule cells (37), the NMDA EPSC decay time slowed down during Mg²⁺ washout more at negative than at positive membrane potentials. We also found this difference for NMDA EPSCs in CA1 synapses for all three genotypes, but to different extents. The slowdown of the NMDA EPSC decay time was more pronounced for wild type than for both NR2 mutants at -40 mV (Fig. 1C). At +40 mV, the decay time of NMDA EPSCs slowed down only for wild-type mice, but remained unchanged for NR2A^{-/-} and NR2B^{ΔFb} mice (Fig. 1C). Thus, removal of Mg²⁺ changed the deactivation kinetics of NMDA EPSCs at negative and positive potentials in wild type, but exclusively at negative potentials and to a lesser extent in both NR2 mutants. To our knowledge, this observation during single-pulse stimulation provides the first evidence that a population of NMDARs distinct from diheteromeric NR1/NR2A and NR1/NR2B receptors contributes to NMDA EPSCs in wild-type hippocampal slices.

Voltage Dependence of NMDA EPSC Decay Time Points to a Minor Contribution of NR1/NR2B Receptors to NMDA EPSCs in Adult Wild-type Synapses—In wild type, Mg²⁺ confers voltage dependence to the decay time of NMDA EPSCs, with slower kinetics at depolarized potentials (38). Even in the absence of Mg²⁺, NMDA EPSCs decay slower at depolarized potentials (37, 39), which has been modeled recently (40). To estimate the voltage dependence of decay for NMDA EPSCs recorded in wild-type, NR2A^{-/-}, and NR2B^{ΔFb} mice, we calculated the -40 mV/+40 mV ratio of the decay time constants using the values illustrated in Fig. 1C. In the presence of Mg²⁺, NMDA EPSCs in NR2A^{-/-} mice displayed a significantly reduced voltage dependence compared with wild-type and NR2B^{ΔFb} mice (Fig. 2A). This genotypic difference was also observed in the absence of Mg²⁺. NMDA EPSCs still decayed slower at positive than at negative potentials in wild-type and NR2B^{ΔFb} mice, whereas the decay time of NMDA EPSCs in NR2A^{-/-} mice was similar at -40 and +40 mV (Fig. 2B). Hence, in the absence as well as presence of Mg²⁺ voltage

dependence of NMDA EPSC decay kinetics is different for pure synaptic diheteromeric NMDARs.

Based on the above observations, pure NR1/NR2A and NR1/NR2B receptors unlikely mix in equal proportions in synapses of wild-type mice because the voltage dependence of NMDA EPSC decay did not occur halfway between that of the pure NR2 subtypes in wild type. Furthermore, NR1/NR2B receptors with their distinct voltage dependence of decay contribute at best to a minor extent to NMDA EPSCs in adult wild-type mice because the voltage dependence of NMDA EPSC decay kinetics is similar for NMDARs in wild-type mice and for NR1/NR2A receptors in *NR2B*^{ΔFb} mice. In contrast, the NMDA EPSC decay time in wild type is intermediate between both NR2 mutants at negative and positive potentials (see above). Thus, in wild type synaptic triheteromeric NR1/NR2A/NR2B receptors mediate NMDA EPSCs with slower deactivation kinetics than diheteromeric NR1/NR2A receptors, but NR1/NR2A/NR2B and NR1/NR2A receptors display similar voltage dependence of decay. In summary, our analysis of voltage dependence and decay time of NMDA EPSCs in three genotypes strongly suggests that NMDA EPSCs elicited by low frequency stimulation in adult CA3-to-CA1 synapses of wild-type mice are mainly mediated by NR1/NR2A and NR1/NR2A/NR2B receptors.

Pharmacology Reveals Presence of NR2B-containing Receptors in CA1 Synapses throughout Development—In addition to characterizing the NMDAR composition in synapses of adult wild-type mice by subtype-specific kinetic properties with the help of NR2A and NR2B mutant mice (Figs. 1 and 2), we next used a pharmacological approach in neonatal *versus* adult mice. The NR2B-directed NMDAR antagonist CP-101,606 (10 μM) reduced NMDA EPSCs in the absence of Mg²⁺ in neonatal wild-type mice by about 65% and in adult mice by about 50% (Fig. 3A and Table 1). Given that NR1/NR2B receptors contributed to NMDA EPSCs only to a minor extent under our experimental conditions in adult hippocampal synapses (Figs. 1 and 2), the 50% reduction by CP-101,606 in adult mice must result from antagonism of NR1/NR2A/NR2B rather than NR1/NR2B receptors. NR1/NR2A/NR2B receptors likely contribute to NMDA EPSCs more than 50%, because CP-101,606 (10 μM) antagonizes recombinant NR1/NR2B receptors in the absence of Mg²⁺ only up to 80–90% (41, 42).

Previous studies demonstrated a developmental decrease in the sensitivity of NR2B-directed NMDAR antagonists in various brain regions (43–47), explained by a postnatal increase in NR2A expression (6, 8, 26, 48). Under our experimental conditions in 0 mM Mg²⁺, the sensitivity of CP-101,606 only moderately decreased during postnatal development and did not change at +40 mV (Fig. 3A). When repeating this experiment in presence of a physiological Mg²⁺ concentration (1 mM), the sensitivity of CP-101,606 significantly decreased at both membrane potentials during postnatal development (Fig. 3B), indicating that recording conditions can influence the sensitivity of CP-101,606 (see also Fig. 4 for experiments in *NR2A*^{−/−} mice).

In cultured cortical neurons, extracellular Mg²⁺ was found to reduce the apparent receptor affinity for ifenprodil (49), the first described NR2B-directed NMDAR antagonist. We used ifenprodil <10 μM, *i.e.* at 3 μM, which provides a selective block of NR2B-containing NMDARs (42). Consistent with

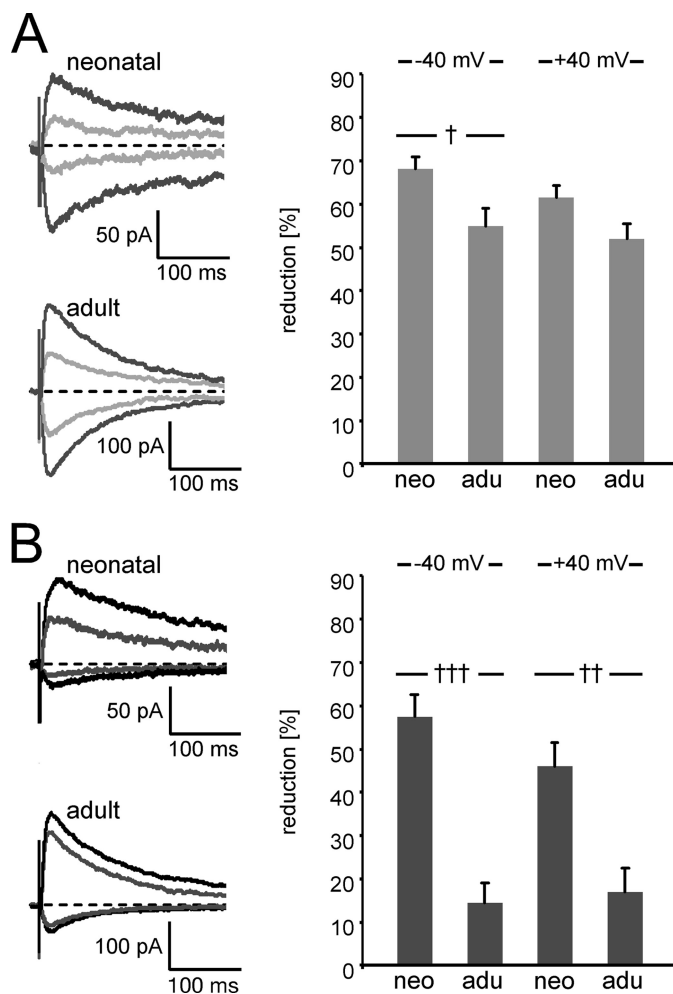


FIGURE 3. Effects of CP-101,606 on NMDA EPSCs in neonatal versus adult wild-type mice. Averaged representative current traces show NMDA EPSCs at −40 and +40 mV in the absence (A, gray) and presence (B, black) of Mg²⁺ before and after (faint gray) perfusion of CP-101,606 (10 μM; 20 min). A, reduction of NMDA EPSCs recorded in Mg²⁺-free Ringer's solution by CP-101,606 for neonatal and adult mice (at −40 mV: neonatal, 68.18 ± 2.89%, *n* = 6; adult, 54.98 ± 4.08%, *n* = 9, *t*, *p* < 0.05 unpaired *t* test; at +40 mV: neonatal, 61.53 ± 2.80%, *n* = 6; adult, 52.0 ± 3.44%, *n* = 9, *p* = 0.07). B, same as A, but in presence of 1 mM Mg²⁺ (at −40 mV: neonatal, 57.47 ± 5.19%, *n* = 7; adult, 14.47 ± 4.45%, *n* = 7, *+++*, *p* < 0.0001 unpaired *t* test; at +40 mV: neonatal, 52.93 ± 8.46%, *n* = 7; adult, 17.0 ± 5.39%, *n* = 7, *++*, *p* < 0.01).

CP-101,606, the sensitivity of ifenprodil did not decrease during postnatal development in the absence of Mg²⁺ either at −40 mV (neonatal, 35.74 ± 9.25%, *n* = 6; adult, 40.03 ± 2.66%, *n* = 7; *p* = 0.68 unpaired *t* test) or at +40 mV (neonatal, 29.94 ± 5.70%, *n* = 6; adult, 39.29 ± 7.52%, *n* = 7; *p* = 0.35 unpaired *t* test). By contrast, the sensitivity of ifenprodil decreased in the presence of Mg²⁺, *i.e.* NMDA EPSCs even increased at both membrane potentials in adult synapses (*p* < 0.0001 unpaired *t* test), at −40 mV (neonatal, 50.70 ± 6.80%, *n* = 9; adult, −38.86 ± 10.14%, *n* = 7) and at +40 mV (neonatal, 52.93 ± 8.46% *n* = 7; adult, −18.61 ± 6.69%, *n* = 7).

In summary, Mg²⁺ influenced the sensitivity of CP-101,606 and ifenprodil. Furthermore, the strong peak reduction of NMDA EPSCs in adult mice in the absence of Mg²⁺ by these two antagonists indicates that NR2B-containing NMDARs remain present in hippocampal synapses throughout postnatal development, reflecting a successive replacement of NR1/

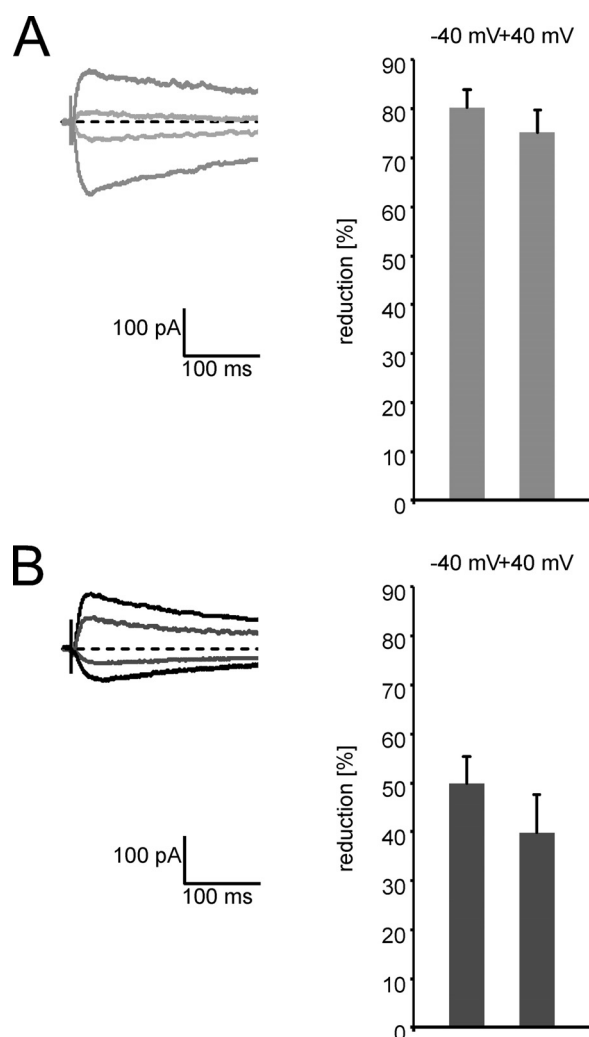


FIGURE 4. Effects of CP-101,606 on NMDA EPSCs in adult $NR2A^{-/-}$ mice. Averaged representative current traces show NMDA EPSCs at -40 and $+40$ mV in the absence (A, gray) and presence (B, black) of Mg^{2+} before and after (faint gray) perfusion of CP-101,606 ($10 \mu M$). A, in Mg^{2+} -free Ringer's solution, CP-101,606 reduced NMDA EPSCs at -40 by $80.33 \pm 3.83\%$ ($n = 7$) and $+40$ mV by $75.13 \pm 4.53\%$ ($n = 7$). B, in the presence of 1 mM Mg^{2+} , reduction of NMDA EPSCs by CP-101,606 was reduced compared with Mg^{2+} -free conditions (-40 mV, $p < 0.001$; $+40$ mV, $p < 0.01$ unpaired t tests; reduction at -40 mV, $49.90 \pm 5.41\%$, $n = 7$; $+40$ mV, $39.71 \pm 7.86\%$, $n = 7$).

NR2B receptors by NR1/NR2A/NR2B receptors. Interestingly, even in cultured neurons, NR1/NR2A/NR2B receptors appear to be specifically targeted to, and incorporated into, nascent synapses (27).

Extracellular Mg^{2+} Concentration and NMDAR Subtype Affect Sensitivity of CP-101,606—Extracellular Mg^{2+} influenced the sensitivity of CP-101,606 (Fig. 3 and Table 1). In neonates, NMDA EPSCs showed a trend to be less inhibited in 1 than in 0 mM extracellular Mg^{2+} ($p = 0.11$ at -40 mV; $p = 0.05$ at $+40$ mV; unpaired t tests), whereas in adult mice, NMDA EPSCs were more reduced in absence than presence of Mg^{2+} ($p < 0.0001$ at -40 mV; $p < 0.001$ at $+40$ mV; unpaired t tests). Thus, the extent of Mg^{2+} influence on CP-101,606 sensitivity may depend on the presence of different NR2B-containing NMDARs in neonatal versus adult synapses.

To investigate the influence of Mg^{2+} on the sensitivity of CP-101,606 independent of NR1/NR2A/NR2B receptors, we

examined the effect of CP-101,606 on NMDA EPSCs in CA1 cells of adult $NR2A^{-/-}$ mice, which contain only NR1/NR2B receptors. In the absence of Mg^{2+} , NMDA EPSCs were reduced by about 80% (Fig. 4A), which is comparable with the maximal antagonism of recombinant NR1/NR2B receptors (80–90%; (Refs. 41 and 42). In the presence of Mg^{2+} , the effect of CP-101,606 was significantly reduced ($p < 0.001$ at -40 mV; $p < 0.01$ at $+40$ mV; unpaired t tests; Fig. 4B). This confirms in $NR2A^{-/-}$ mice that the sensitivity of CP-101,606 is enhanced in the absence of Mg^{2+} . Because the reduction of the CP effect by Mg^{2+} is more pronounced for NMDARs in adult wild-type than for NR1/NR2B receptors in $NR2A^{-/-}$ mice ($p < 0.001$ unpaired t test, Fig. 3 versus $p < 0.01$ unpaired t test, Fig. 4), the absence of Mg^{2+} seems to strengthen the antagonism by CP-101,606 even more for triheteromeric NMDARs. Thus, antagonism is reduced by presence of NR2A (27, 50, 51) and also by the presence of Mg^{2+} , as shown in Figs. 3 and 4 (see also 49).

DISCUSSION

Key to this study was the analysis of voltage dependence of NMDA EPSC decay time in combination with the use of NR2B-directed NMDAR antagonists in the absence of Mg^{2+} in acute hippocampal slices of wild-type and two lines of gene-targeted mice, $NR2A^{-/-}$ and $NR2B^{\Delta Fb}$ mice. Our results ascertain the presence of NR2B-containing NMDARs in CA3-to-CA1 synapses throughout development and identify triheteromeric NR1/NR2A/NR2B receptors as a prominent NMDAR population in CA1 synapses of adult wild-type mice.

Triheteromeric NMDARs form without doubt, but testing their relative abundance and relative distribution within and outside synapses is delicate. Biochemical approaches analyzing membrane fractions yielded different amounts of triheteromeric NMDARs even within the same brain structure (23–26, 29) because of technical limitations shared among all biochemical studies of NMDARs as discussed in the most recent study (29). To identify different NMDAR subtypes within distinct circuits, e.g. in CA3-to-CA1 synapses, electrophysiologists usually test the sensitivity of NMDA EPSCs to NMDAR antagonists, which were primarily characterized for recombinant diheteromeric NMDARs. This approach allows conclusions regarding NR2B-containing (NR2B-type) NMDARs but lacks a rigorous distinction between di- and triheteromeric NMDARs. During the first postnatal week, NMDA EPSCs in CA1 neurons are highly sensitive to NR2B-directed NMDAR antagonists (our study; 44–47). In adult wild-type mice, our experiments show that CP-101,606 reduced NMDA EPSCs about 50%. Similarly, ifenprodil and its derivative Ro25-6981 reduced NMDA EPSCs in adult mice by approximately 40% (our study; 39, 52–56). Thus, experiments with NR2B-specific antagonists support that NR2B-containing NMDARs remain present in hippocampal synapses throughout development.

The presence of NR2B in adult hippocampal synapses is consistent with previous studies (12–15) and with our analysis of the NMDA EPSC decay time following single-pulse stimulation in acute slices of the three genotypes. In the absence of Mg^{2+} , synaptic NR1/NR2B receptors deactivated 6–9-fold slower than synaptic NR1/NR2A receptors, the decay time of NMDA

EPSCs in adult wild-type mice was 2–3-fold slower than the respective decay time for NR1/NR2A receptors in *NR2B^{ΔFb}* mice. Thus, the NMDA EPSC decay time in wild type was not halfway of that of the diheteromeric NMDARs and argues against a 50% contribution of NR1/NR2B receptors to NMDA EPSCs in wild type. Certainly, our demonstration that the voltage dependence of NMDA EPSC decay is distinct for NR1/NR2B and NR1/NR2A receptors in the absence and presence of Mg^{2+} argues for a definite presence of NR1/NR2A/NR2B receptors in adult synapses. If NR1/NR2B receptors were approximately 50% (to predominate) in adult wild-type hippocampal synapses, their distinct voltage dependence of decay would have caused a bigger $-40/+40$ mV ratio of decay time constants than observed. In fact, the voltage dependence of decay is not significantly different in adult wild-type and *NR2B^{ΔFb}* mice. Consequently, the NR2B-containing receptors in CA1 synapses of adult wild-type mice represent mainly NR1/NR2A/NR2B receptors. These receptors mediate NMDA EPSCs with slower deactivation kinetics than NR1/NR2A receptors reminiscent of NR2B but at the same time exhibit the NR1/NR2A characteristic voltage dependence of decay. Thus, presence of NR2B in NR1/NR2A/NR2B receptors slows the deactivation, whereas presence of NR2A confers the voltage dependence of decay. This arrangement in triheteromeric NMDARs generated a new property of NMDARs that cannot be explained by a mixture of diheteromeric NR1/NR2A and NR1/NR2B receptors.

Outside synapses, live surface labeling detected a similar distribution of NR2A and NR2B (57), which may reflect the finding of a recent quantitative biochemical study, showing that NR1/NR2A, NR1/NR2B, and NR1/NR2A/NR2B receptors each constituted approximately one-third of the total NMDAR population at P7, P42, and 6 months (29). On the other hand, constant proportions of the three NMDAR subtypes throughout development in whole hippocampus are not in agreement with the increasing NR2A/NR2B ratio during development (6, 7, 48). In particular, the synaptic NMDAR content changes during development and is indicated by two facts, as reported in this and previous studies: (i) the decay time constant of NMDA EPSCs decreases during development because of the increasing NR2A expression and (ii) the sensitivity to NR2B-directed NMDAR antagonists usually decreases (for review, see *e.g.* Ref. 58).

We also observed a developmental decrease in the antagonist sensitivity of ifenprodil and CP-101,606 in wild-type mice as long as we recorded NMDA EPSCs in the presence of Mg^{2+} . This was not observed in the absence of Mg^{2+} and suggested that recording conditions influence the sensitivity of both NR2B-directed NMDAR antagonists in slices. We confirmed this possibility for CP-101,606 in adult *NR2A^{-/-}* mice, which lack NR1/NR2A and NR1/NR2A/NR2B receptors, by showing that NMDA EPSCs were antagonized by CP-101,606 more strongly in the absence than presence of Mg^{2+} . This influence of Mg^{2+} appears to be restricted to native NMDAR channels (our results; 49) because ifenprodil antagonized recombinant NR1/NR2B receptors to similar extents in the absence and presence of Mg^{2+} (51). Yet, the 80% reduction of NR1/NR2B receptor-mediated NMDA EPSCs by CP-101,606 observed

under Mg^{2+} -free conditions ($\leq 4.5 \mu M$) is close to the maximal (80–90%) reduction of agonist currents mediated by recombinant NR1/NR2B receptors (41, 42). Thus, to achieve maximal antagonism by NR2B-directed NMDAR antagonists in slices, the absence of Mg^{2+} is recommended. This is particularly important when triheteromeric NMDARs are present because in the presence of Mg^{2+} antagonism by CP-101,606 of NR1/NR2A/NR2B receptors is more constrained than that of NR1/NR2B receptors. This latter conclusion is based on the observation that the reduced sensitivity of CP-101,606 in presence of Mg^{2+} was more pronounced in wild-type than in *NR2A^{-/-}* mice ($p < 0.001$ unpaired *t* test, Fig. 3 *versus* $p < 0.01$ unpaired *t* test, Fig. 4).

In heterologous cells, ifenprodil binds with high affinity to both NR1/NR2B and NR1/NR2A/NR2B receptors, but currents mediated by these subtypes are reduced to different extents. NR1/NR2A/NR2B receptors were reduced by about 20% (51), whereas NR1/NR2B receptors were maximally inhibited, which is 80–90% (41, 42). This low sensitivity of recombinant triheteromeric NMDARs for ifenprodil (51) may be enhanced for the ifenprodil derivatives, CP-101,606 and Ro25-6981, which have higher affinity for NR1/NR2B receptors than ifenprodil (42, 59, 60), but this possibility remains to be tested electrophysiologically on recombinant NR1/NR2A/NR2B receptors. CP-101,606 and Ro25-6981 were previously proposed to represent two classes of NR2B-directed NMDAR antagonists (59). Ro25-6981 was found to bind with similarly high affinities to both NR1/NR2B and NR1/NR2A/NR2B receptors (61), whereas binding of CP-101,606 was significantly reduced by the presence of another NR2 subunit within recombinant NMDAR complexes (59). Unfortunately, this distinction did not apply when examining the sensitivity of NMDA EPSCs to CP-101,606. In adult hippocampal synapses, the 50% reduction of NMDA EPSCs by CP-101,606 that we observed in the absence of Mg^{2+} and others observed with ifenprodil and Ro25-6981 in absence or presence of Mg^{2+} (39, 52–56) strongly suggests that NR2B-directed NMDAR antagonists block NR1/NR2A/NR2B receptors in neurons $>20\%$ because NR1/NR2B receptors contribute to a minor extent to NMDA EPSCs at this developmental stage. In summary, ifenprodil and its derivatives are NR2B-directed but not NR1/NR2B-selective antagonists. Furthermore, the 50% reduction of NMDA EPSCs by CP-101,606 identifies triheteromeric NMDARs as the foremost NMDAR subtype in adult synapses.

The existence of triheteromeric NMDARs in adult mice raises the question as to their function. Because it is impossible to examine this NMDAR population in isolation, the role of NR1/NR2A/NR2B receptors remains speculative. Regarding synaptic plasticity, the magnitude of NMDAR-dependent LTP and charge transfer during induction by low frequency stimulation correlate in hippocampal synapses of 4–7-week-old mice (31, 62). The presence of NR2B in *NR2A^{-/-}* mice preserves LTP (62, 63), and the lack of NR2B in CA1 neurons of *NR2B^{ΔFb}* mice impairs LTP and memory (31), indicating that the presence of NR2B within NR1/NR2A/NR2B receptors in adult wild-type mice is crucial for charge transfer during hippocampal LTP induction, learning, and memory. Furthermore, the presence of NR2B within synaptic NMDARs could be essential

at all developmental stages for the following reasons. NR2B appears to play a dominant role in the trafficking of NR2A/NR2B-containing NMDARs *in vivo* (64), and NR2B compared with NR2A allows binding with higher affinity to molecules important for NMDAR signaling, e.g. CaMKII (14, 65, 66), ras-GRF1 (67), and SynGAP (68).

Acknowledgments—We thank Drs. S. Astori, S. Berberich, O. Hvalby, J. W. Johnson, P. H. Seeburg, and M. Trevino for valuable comments on the manuscript; Dr. A. Kopp-Schneider for statistical advice; and Dr. P. H. Seeburg for generous support. We also thank Dr. M. Mishina for providing the NR2A^{-/-} mouse line and Dr. H. Monyer for providing NR2B^{ΔFb} mice.

REFERENCES

- Dingledine, R., Borges, K., Bowie, D., and Traynelis, S. F. (1999) *Pharmacol. Rev.* **51**, 7–61
- Nakazawa, K., McHugh, T. J., Wilson, M. A., and Tonegawa, S. (2004) *Nat. Rev. Neurosci.* **5**, 361–372
- Rothman, S. M., and Olney, J. W. (1995) *Trends Neurosci.* **18**, 57–58
- Rambhadrar, A., Gonzalez, J., and Jayaraman, V. (2010) *J. Biol. Chem.* **285**, 15296–15301
- Sobolevsky, A. I., Rosconi, M. P., and Gouaux, E. (2009) *Nature* **462**, 745–756
- Monyer, H., Burnashev, N., Laurie, D. J., Sakmann, B., and Seeburg, P. H. (1994) *Neuron* **12**, 529–540
- Watanabe, M., Inoue, Y., Sakimura, K., and Mishina, M. (1993) *J. Comp. Neurol.* **338**, 377–390
- Wenzel, A., Fritschy, J. M., Mohler, H., and Benke, D. (1997) *J. Neurochem.* **68**, 469–478
- Costa, B. M., Feng, B., Tsintsadze, T. S., Morley, R. M., Irvine, M. W., Tsintsadze, V., Lozovaya, N. A., Jane, D. E., and Monaghan, D. T. (2009) *J. Pharmacol. Exp. Ther.* **331**, 618–626
- Harney, S. C., Jane, D. E., and Anwyl, R. (2008) *J. Neurosci.* **28**, 11685–11694
- Lozovaya, N. A., Grebenyuk, S. E., Tsintsadze, T. S., Feng, B., Monaghan, D. T., and Krishtal, O. A. (2004) *J. Physiol.* **558**, 451–463
- Goebel-Goody, S. M., Davies, K. D., Alvestad Linger, R. M., Freund, R. K., and Browning, M. D. (2009) *Neuroscience* **158**, 1446–1459
- Köhr, G., Jensen, V., Koester, H. J., Mihaljevic, A. L., Utvik, J. K., Kvello, A., Ottersen, O. P., Seeburg, P. H., Sprengel, R., and Hvalby, Ø. (2003) *J. Neurosci.* **23**, 10791–10799
- Zhou, Y., Takahashi, E., Li, W., Halt, A., Wiltgen, B., Ehninger, D., Li, G. D., Hell, J. W., Kennedy, M. B., and Silva, A. J. (2007) *J. Neurosci.* **27**, 13843–13853
- Shinohara, Y., Hirase, H., Watanabe, M., Itakura, M., Takahashi, M., and Shigemoto, R. (2008) *Proc. Natl. Acad. Sci. U.S.A.* **105**, 19498–19503
- Cull-Candy, S. G., and Leszkiewicz, D. N. (2004) *Sci. STKE* **255**, re16
- Mony, L., Kew, J. N., Gunthorpe, M. J., and Paoletti, P. (2009) *Br. J. Pharmacol.* **157**, 1301–1317
- Yashiro, K., and Philpot, B. D. (2008) *Neuropharmacology* **55**, 1081–1094
- Collingridge, G. L., Isaac, J. T., and Wang, Y. T. (2004) *Nat. Rev. Neurosci.* **5**, 952–962
- Liu, Y., Wong, T. P., Aarts, M., Rooyackers, A., Liu, L., Lai, T. W., Wu, D. C., Lu, J., Tymianski, M., Craig, A. M., and Wang, Y. T. (2007) *J. Neurosci.* **27**, 2846–2857
- Martel, M. A., Wyllie, D. J., and Hardingham, G. E. (2009) *Neuroscience* **158**, 334–343
- von Engelhardt, J., Coserea, I., Pawlak, V., Fuchs, E. C., Köhr, G., Seeburg, P. H., and Monyer, H. (2007) *Neuropharmacology* **53**, 10–17
- Chazot, P. L., Coleman, S. K., Cik, M., and Stephenson, F. A. (1994) *J. Biol. Chem.* **269**, 24403–24409
- Kew, J. N., Richards, J. G., Mutel, V., and Kemp, J. A. (1998) *J. Neurosci.* **18**, 1935–1943
- Luo, J., Wang, Y., Yasuda, R. P., Dunah, A. W., and Wolfe, B. B. (1997) *Mol. Pharmacol.* **51**, 79–86
- Sheng, M., Cummings, J., Roldan, L. A., Jan, Y. N., and Jan, L. Y. (1994) *Nature* **368**, 144–147
- Tovar, K. R., and Westbrook, G. L. (1999) *J. Neurosci.* **19**, 4180–4188
- Brickley, S. G., Misra, C., Mok, M. H., Mishina, M., and Cull-Candy, S. G. (2003) *J. Neurosci.* **23**, 4958–4966
- Al-Hallaq, R. A., Conrads, T. P., Veenstra, T. D., and Wenthold, R. J. (2007) *J. Neurosci.* **27**, 8334–8343
- Sakimura, K., Kutsuwada, T., Ito, I., Manabe, T., Takayama, C., Kushiya, E., Yagi, T., Aizawa, S., Inoue, Y., Sugiyama, H., and et al. (1995) *Nature* **373**, 151–155
- von Engelhardt, J., Doganci, B., Jensen, V., Hvalby, Ø., Göngrich, C., Taylor, A., Barkus, C., Sanderson, D. J., Rawlins, J. N., Seeburg, P. H., Bannerman, D. M., and Monyer, H. (2008) *Neuron* **60**, 846–860
- Stocca, G., and Vicini, S. (1998) *J. Physiol.* **507**, 13–24
- Zhang, W., Howe, J. R., and Popescu, G. K. (2008) *Nat. Neurosci.* **11**, 1373–1375
- Vicini, S., Wang, J. F., Li, J. H., Zhu, W. J., Wang, Y. H., Luo, J. H., Wolfe, B. B., and Grayson, D. R. (1998) *J. Neurophysiol.* **79**, 555–566
- Kuner, T., and Schoepfer, R. (1996) *J. Neurosci.* **16**, 3549–3558
- Kutsuwada, T., Sakimura, K., Manabe, T., Takayama, C., Katakura, N., Kushiya, E., Natsume, R., Watanabe, M., Inoue, Y., Yagi, T., Aizawa, S., Arakawa, M., Takahashi, T., Nakamura, Y., Mori, H., and Mishina, M. (1996) *Neuron* **16**, 333–344
- Konnerth, A., Keller, B. U., Ballanyi, K., and Yaari, Y. (1990) *Exp. Brain Res.* **81**, 209–212
- Hestrin, S. (1992) *Nature* **357**, 686–689
- Kirson, E. D., and Yaari, Y. (1996) *J. Physiol.* **497**, 437–455
- Clarke, R. J., and Johnson, J. W. (2008) *J. Physiol.* **586**, 5727–5741
- Mott, D. D., Doherty, J. J., Zhang, S., Washburn, M. S., Fendley, M. J., Lyuboslavsky, P., Traynelis, S. F., and Dingledine, R. (1998) *Nat. Neurosci.* **1**, 659–667
- Williams, K. (1993) *Mol. Pharmacol.* **44**, 851–859
- Barth, A. L., and Malenka, R. C. (2001) *Nat. Neurosci.* **4**, 235–236
- Bellone, C., and Nicoll, R. A. (2007) *Neuron* **55**, 779–785
- Brothwell, S. L., Barber, J. L., Monaghan, D. T., Jane, D. E., Gibb, A. J., and Jones, S. (2008) *J. Physiol.* **586**, 739–750
- de Marchena, J., Roberts, A. C., Middlebrooks, P. G., Valakh, V., Yashiro, K., Wilfley, L. R., and Philpot, B. D. (2008) *J. Neurophysiol.* **100**, 1936–1948
- Lopez de Armentia, M., and Sah, P. (2003) *J. Neurosci.* **23**, 6876–6883
- Sans, N., Petralia, R. S., Wang, Y. X., Blahos, J., 2nd, Hell, J. W., and Wenthold, R. J. (2000) *J. Neurosci.* **20**, 1260–1271
- Kew, J. N., and Kemp, J. A. (1998) *J. Physiol.* **512**, 17–28
- Brimecombe, J. C., Boeckman, F. A., and Aizenman, E. (1997) *Proc. Natl. Acad. Sci. U.S.A.* **94**, 11019–11024
- Hatton, C. J., and Paoletti, P. (2005) *Neuron* **46**, 261–274
- Kawakami, R., Dobi, A., Shigemoto, R., and Ito, I. (2008) *PLoS One* **3**, e1945
- Kawakami, R., Shinohara, Y., Kato, Y., Sugiyama, H., Shigemoto, R., and Ito, I. (2003) *Science* **300**, 990–994
- Martina, M., B-Turcotte, M. E., Halman, S., Tsai, G., Tiberi, M., Coyle, J. T., and Bergeron, R. (2005) *J. Physiol.* **563**, 777–793
- Scimemi, A., Fine, A., Kullmann, D. M., and Rusakov, D. A. (2004) *J. Neurosci.* **24**, 4767–4777
- Tang, T. T., Yang, F., Chen, B. S., Lu, Y., Ji, Y., Roche, K. W., and Lu, B. (2009) *Proc. Natl. Acad. Sci. U.S.A.* **106**, 21395–21400
- Petralia, R. S., Wang, Y. X., Hua, F., Yi, Z., Zhou, A., Ge, L., Stephenson, F. A., and Wenthold, R. J. (2010) *Neuroscience* **167**, 68–87
- Köhr, G. (2006) *Cell Tissue Res.* **326**, 439–446
- Chazot, P. L., Lawrence, S., and Thompson, C. L. (2002) *Neuropharmacology* **42**, 319–324
- Fischer, G., Mutel, V., Trube, G., Malherbe, P., Kew, J. N., Mohacs, E., Heitz, M. P., and Kemp, J. A. (1997) *J. Pharmacol. Exp. Ther.* **283**, 1285–1292
- Hawkins, L. M., Chazot, P. L., and Stephenson, F. A. (1999) *J. Biol. Chem.* **274**, 27211–27218
- Berberich, S., Jensen, V., Hvalby, Ø., Seeburg, P. H., and Köhr, G. (2007) *Neuropharmacology* **52**, 77–86

Molecular Composition of Synaptic NMDA Receptors

- 63. Kiyama, Y., Manabe, T., Sakimura, K., Kawakami, F., Mori, H., and Mishina, M. (1998) *J. Neurosci.* **18**, 6704–6712
- 64. Tang, T. T., Badger, J. D., 2nd, Roche, P. A., and Roche, K. W. (2010) *J. Biol. Chem.* **285**, 20975–20981
- 65. Barria, A., and Malinow, R. (2005) *Neuron* **48**, 289–301
- 66. Bayer, K. U., De Koninck, P., Leonard, A. S., Hell, J. W., and Schulman, H. (2001) *Nature* **411**, 801–805
- 67. Krapivinsky, G., Krapivinsky, L., Manasian, Y., Ivanov, A., Tyzio, R., Pellegrino, C., Ben-Ari, Y., Clapham, D. E., and Medina, I. (2003) *Neuron* **40**, 775–784
- 68. Kim, M. J., Dunah, A. W., Wang, Y. T., and Sheng, M. (2005) *Neuron* **46**, 745–760